Mott-Anderson transition controlled by a magnetic field in pyrochlore molybdate

N. Hanasaki, M. Kinuhara, István Kézsmárki, S. Iguchi, S. Miyasaka, N. Takeshita, C. Terakura, H. Takagi, Y. Tokura

Angaben zur Veröffentlichung / Publication details:

Hanasaki, N., M. Kinuhara, István Kézsmárki, S. Iguchi, S. Miyasaka, N. Takeshita, C. Terakura, H. Takagi, and Y. Tokura. 2006. "Mott-Anderson transition controlled by a magnetic field in pyrochlore molybdate." *Physical Review Letters* 96 (11): 116403. https://doi.org/10.1103/physrevlett.96.116403.

Mott-Anderson Transition Controlled by a Magnetic Field in Pyrochlore Molybdate

N. Hanasaki,[1] M. Kinuhara,[1] I. Kézsmárki,[1] S. Iguchi,[2] S. Miyasaka,[1] N. Takeshita,[3] C. Terakura,[3] H. Takagi,[3,4] and Y. Tokura[1,2,3]

[1]*Department of Applied Physics, University of Tokyo, Tokyo 113-8656, Japan*
[2]*Spin Superstructure Project, ERATO, Japan Science and Technology Agency, Tsukuba 305-8562, Japan*
[3]*Correlated Electron Research Center (CERC), National Institute of Advanced Industrial Science and Technology (AIST), Tsukuba 305-8562, Japan*
[4]*Department of Advanced Materials Science, University of Tokyo, Kashiwa 277-8581, Japan*

(Received 13 July 2005; published 24 March 2006)

The pyrochlore molybdate $Gd_2Mo_2O_7$ locates near the phase boundary between the ferromagnetic-metallic and the spin-glass insulating state. This metal-insulator transition is governed on a large energy scale by the electron-correlation effect, while the geometrical frustration causes the random potential. The magnetic field can tune the randomness of the potential and control, under a suitable pressure, the continuous Mott-Anderson transition precisely. The critical exponent ($\mu = 1.04 \pm 0.1$) of the Mott-Anderson transition has been determined for this ferromagnetic orbital-degenerate electron system.

DOI: 10.1103/PhysRevLett.96.116403 PACS numbers: 71.30.+h, 71.27.+a

The metal-insulator transition has been one of central topics in the physics of correlated electron systems [1]. In the Mott transition, the on site Coulomb interaction creates the strongly renormalized quasiparticle state or opens the charge gap (Mott gap) at the Fermi level [2,3]. The transition occurs in a discontinuous manner and the first-order phase boundary terminates at a second-order critical point [4–6]. On the other hand, in the Anderson transition, which is continuous even at zero temperature, the disorder causes the localization of the electrons, which form finite density of states at the Fermi level but cannot contribute to the conduction [7]. The scaling theory has advanced the understanding of the metal-insulator transition: The critical exponent of the transition is determined by the symmetry of the electron system and the universality class [8–10]. The critical exponent μ for the conductivity is defined as $\sigma \sim (x - x_c)^{\mu}$, where x is a control parameter for the metal-insulator transition. In the case of noninteracting electrons, the theoretical studies on the Anderson transition suggest the critical exponent $\mu = 1.4$–1.6 [11]. The scaling theory is also applicable to the Mott transition [1,4,5]. Recently, Limelette *et al.* have succeeded in applying the finite-temperature scaling to the first-order Mott transition, and estimated the critical exponent as $\mu = 0.33$ [4]. Kagawa *et al.* have reported the criticality of the Mott transition in two-dimensional organic material [5,6]. In the case in which both effects are present, the quantitative nature of the metal-insulator transition, the Mott-Anderson transition, remains as an open problem [12–15]. The critical exponent for the Mott-Anderson transition is still puzzling owing to the difficulty in performing precise experiments. For the proper scaling analysis, it is necessary to fine-tune a control parameter driving the Mott-Anderson transition, while keeping the others unchanged. Many experimental reports have suggested different values of the critical exponent, most of which were determined by the comparison between the conductivity values in the different samples [8], and hence possibly affected by the difference in quality between the samples.

In this Letter, we report the nature of the Mott-Anderson transition in the pyrochlore molybdate and its critical behavior determined by the finite-temperature scaling analysis. $Gd_2Mo_2O_7$ is located in the vicinity of the Mott-Anderson transition. The magnetic field can control directly the magnitude of the random potential and hence precisely the metal-insulator transition, while application of high pressure can also prepare the critical state close to the transition. Both methods offer clear experiment for tuning the two control parameters of the Mott-Anderson transition, i.e., the bandwidth and the random potential. In this study, we can avoid the ambiguity due to the difference in quality and stoichiometry among the samples.

In $R_2Mo_2O_7$, the pyrochlore lattice has two sublattices of the rare earth R site and the Mo site, which are displaced by half a unit cell [16]. In these sublattices, the ions locate at the vertex of the corner-sharing tetrahedra. The trigonal crystal field splits the t_{2g} manifold of the Mo site into a_{1g} and the degenerate e_g' states. In $R_2Mo_2O_7$ with the $4d^2$ configuration of Mo, one electron populates the a_{1g} orbital and another the e_g' orbital. The e_g'-state electrons contribute to the conduction, while the a_{1g}-state electrons give the local moments. The Hund's rule couples ferromagnetically the spins in the e_g' orbital and a_{1g} orbital, stabilizing the half-metallic state [17].

It was reported that $R_2Mo_2O_7$ shows the ferromagnetic-metallic ground state for the larger-radius rare earth R ions (R = Nd and Sm) than Gd ion, while a spin-glass insulating state appears for the smaller R ions (R = Dy, Ho, and Y) [18–20]. Towards the larger rare-earth radius, the Mo-O-Mo bond angle (or equivalently the transfer energy) is increased [21], and hence tends to stabilize the metallic state via the double-exchange interaction. In contrast, in the case where the interorbital on site Coulomb interaction

in the degenerate e_g' orbitals exceeds the transfer energy, it may lead to the Mott insulator [17]. In the Mott-insulating state, the antiferromagnetic superexchange interaction is dominant between the Mo sites [17], which yields the spin-glass state because of the spin frustration on the pyrochlore lattice. In the insulating Dy and Ho compound, the clear Mott gap is observed in the optical spectra [19,22]. In the phase diagram of the $R_2Mo_2O_7$ family as a function of the R ionic radius, the $Gd_2Mo_2O_7$ compound is located on the verge of the metal-insulator transition with almost zero gap, $\Delta \approx 20$ meV [22]. The systematic change of the ground-state optical spectra suggests a quantum phase transition occurring around $Gd_2Mo_2O_7$, in which a competition between the spin-glass phase and the ferromagnetic phase is involved. The Raman spectra show the enhancement of the carrier mass as the metal-insulator transition boundary is approached from the metallic side [23].

A single crystal was grown by the floating-zone method in an Ar atmosphere. Transport properties of $Gd_2Mo_2O_7$ are known to be sensitive to oxygen off stoichiometry, that may even produce the metallic state, perhaps due to an effective carrier-doping process. We investigate a well stoichiometric, namely, most insulating, $Gd_2Mo_2O_7$ compound. We used a cubic-anvil cell and modified Bridgman-anvil cell [24], which enable the resistivity measurements under the temperature-pressure conditions, (3 –300 K, 0–10 GPa) and (200 mK–20 K, 0–8 GPa), respectively. We set the modified Bridgman-anvil cell in a dilution refrigerator equipped with a superconducting magnet (8 T).

Figure 1 shows the temperature dependence of resistivity of $Gd_2Mo_2O_7$ for various pressures up to 10 GPa. At ambient pressure, where the Mott-insulating state is realized, the resistivity, much higher than the Ioffe-Regel limit ($\rho \sim 5 \times 10^{-4}$ Ω cm), increases with lowering temperature in the whole temperature range. By the application of pressure, the resistivity is effectively decreased. In the intermediate pressure range of ~2–4 GPa, the resistivity curves become nonmonotonous and broad maximums are observed below 300 K, as indicated by the arrows in Fig. 1. These peaks correspond to the coherent-incoherent crossover of the quasiparticle dynamics generic to the correlated electron systems [2,3,22]. This peak temperature, below which the coherent quasiparticle state is formed, gradually increases with the pressure. The conductivity under various pressures is plotted in Fig. 2 as a function of the square-root of temperature ($T^{0.5}$). The open and closed circles represent the data obtained by the cubic-anvil cell and the modified Bridgman-anvil cell, respectively. The conductivity below 20 K is approximately proportional to $T^{0.5}$. The zero-temperature conductivity obtained by the linear extrapolation (straight lines) is plotted as a function of pressure in the inset of Fig. 2. The zero-temperature conductivity shows a continuous onset around 2.4 GPa, above which the finite conductivity is nearly proportional to the pressure. Thus, the pressure or the increment of the transfer energy induces the *continuous* metal-insulator transition

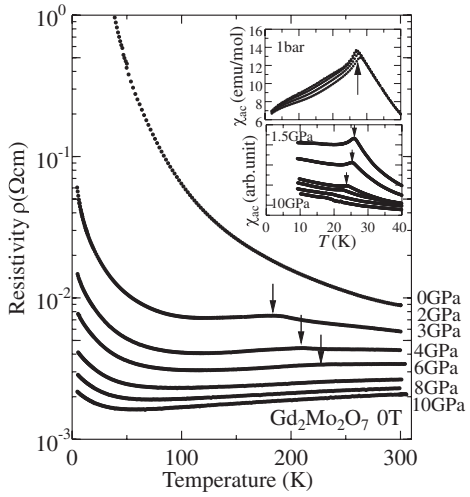

FIG. 1. Temperature dependence of resistivity measured at ambient pressure and high pressures (in the cubic-anvil cell) for $Gd_2Mo_2O_7$. The arrows indicate the resistivity peak signaling the coherent-incoherent crossover of the quasiparticle dynamics. Upper inset: ac magnetic susceptibility and its frequency dependence (from top to bottom; 11, 97, 990 Hz, and 9.9 kHz) measured by the magnetic-field amplitude of 3 Gauss at ambient pressure. The arrow indicates the magnetic anomaly. Lower inset: ac susceptibility measured under high pressures (from top to bottom; 1.5, 2, 3, 4, 6, 8, and 10 GPa) at 3.3 kHz.

around 2.4 GPa even in the absence of an external magnetic field.

At this stage, it is worth characterizing a magnetism of $Gd_2Mo_2O_7$. The inset of Fig. 3(a) shows the temperature dependence of inverse magnetization. The positive Weiss temperature ($\theta = 47.6$ K) suggests the ferromagnetic interaction between the Mo moments. The upper inset of Fig. 1 depicts the ac magnetic susceptibility measured at ambient pressure. The magnetic anomaly observed at 27 K, as indicated by the arrow, shows the clear frequency de-

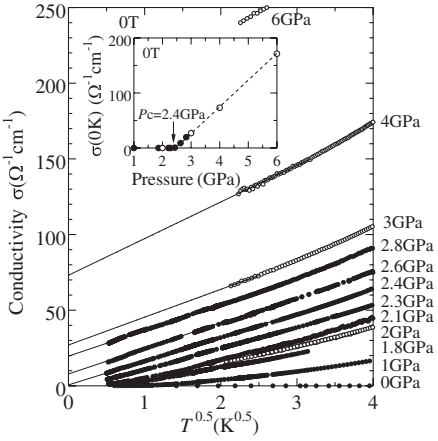

FIG. 2. Conductivity σ plotted as a function of the square root of temperature ($T^{0.5}$) under various pressures. The solid lines are guides for the eye. Inset: Pressure dependence of the zero-temperature conductivity.

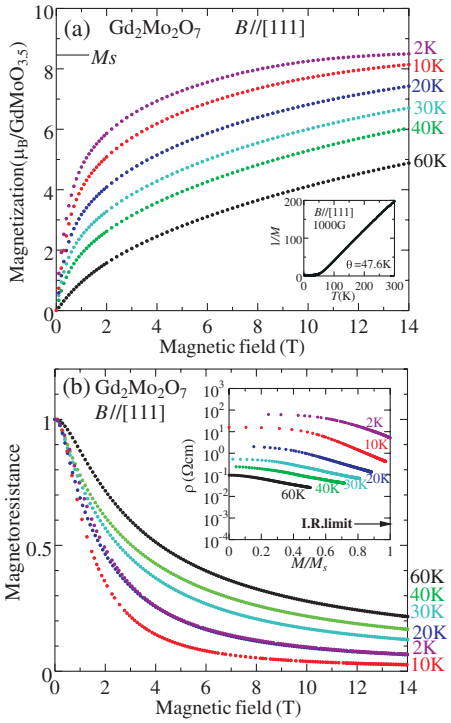

FIG. 3 (color online). (a) Magnetic-field dependence of the magnetization for the field along the [111] direction at ambient pressure. The left horizontal bar indicates the full moment M_s per a chemical unit $GdMoO_{3.5}$. Inset: Inverse of magnetization $[M(\mu_B/GdMoO_{3.5})]$ plotted as a function of temperature (T). (b) Isothermal magnetoresistance (normalized by the zero-field resistance value) for the field along the [111] direction at ambient pressure. Inset: Resistivity plotted as a function of the normalized magnetization M/M_s. The horizontal arrow indicates the Ioffe-Regel (I.R.) limit value of the resistivity.

pendence characteristic of the spin-glass transition, which appears to reflect the antiferromagnetic interaction between the Gd sites in the pyrochlore structure [25]. As displayed in the lower inset, this magnetic anomaly subsists, while gradually fading out, up to the higher pressures. Figure 3(a) displays the magnetization in the magnetic field along the [111] direction at ambient pressure. The increment of magnetization with the magnetic field is saturated at the lowest temperature. Given the Heisenberg-type nature of Gd spin, the contribution of the Gd moment is $7(\mu_B/GdMoO_{3.5})$. According to the previous study [16], the Mo moment was estimated as $\approx 1.4(\mu_B/GdMoO_{3.5})$. Thus, we can estimate the full moment as $M_s = 8.4(\mu_B/GdMoO_{3.5})$, as indicated by the left bar. At the lowest temperature $T = 2$ K, the high-field magnetization is indeed saturated and in $B = 14$ T it is nearly equal to M_s, confirming that the Gd and Mo spins are aligned parallel to each other by the external field. It is reasonable to consider the ferromagnetic coupling between the Mo moments and the Gd moments under high magnetic fields. Thus, the spin frustration, which contributes to the frequency dependence of the magnetic anomaly shown in Fig. 1, appears to be completely suppressed by the high magnetic fields [25].

To exemplify the strong coupling between the transport and the spin configuration, we show in Fig. 3(b) the gigantic negative magnetoresistance observed at ambient pressure. The resistance decreases with magnetic field, more dramatically at lower temperatures. The magnetic field, which aligns both Mo and Gd moments up to the nearly full moment value at low temperatures, decreases the randomness of the potential on the Mo sites and increases the transfer energy by the reduction of the tilting angle between the Mo spins, leading to the large negative magnetoresistance. Therefore, the magnetic field can be a control parameter that drives the Mott-Anderson transition in the present case and has much better controllability and precision than the external pressure. The inset of Fig. 3(b) shows the resistance replotted as a function of the magnetization M at ambient pressure. As increasing M, the resistance decreases. At 2 K and 14 T, the magnetization reaches the value M_s of the full magnetization, and the random potential is expected to be nearly completely suppressed. Nevertheless, the resistivity is still several orders of magnitude larger than the Ioffe-Regel limit ($\rho \sim 5 \times 10^{-4}$ Ω cm). Therefore, the compound appears to remain as the Mott insulator at ambient pressure even in the clean limit. The presence of the Mott gap reduces the dependence of the magnetoresistance on the randomness at low temperatures (<10 K), leading to the apparent minimum of the magnetoresistance around 10 K. Nevertheless, even in the clean limit ($B \rightarrow \infty$), the resistivity appears to keep on increasing monotonously as decreasing temperature. Thus, we need to investigate the transport under high pressures with varying magnetic fields, to precisely control the Mott-Anderson transition.

Figure 4 displays the T dependence of conductivity measured at 1.8 GPa, while changing the magnetic field. The conductivity, proportional to $T^{0.5}$, is continuously increased by applying the magnetic field. The extrapolated zero-temperature conductivity reaches a finite value above $B \approx 2.25$ T, indicating the Mott-Anderson transition. Importantly, this metal-insulator transition at zero temperature appears to be continuous [15,26], as contrasted by the first-order Mott transition in Cr-doped V_2O_3 [4] and in κ-(BEDT-TTF)$_2$Cu[N(CN)$_2$]Cl [5]. On the basis of the magnetoconductivity data of Fig. 4(a), we performed the finite-temperature scaling analysis [8] as shown in Fig. 4(b). All the experimental data fall onto a single curve representing the scaling function $\sigma/T^{\alpha} = f(|1 - B/B_c|/T^{\beta})$ with the parameters $\alpha = 0.50$ and $\beta = 1/\nu z = 0.48$. Here, ν and z denote the critical exponent for the correlation length and the dynamical critical exponent, respectively. By this analysis, we could obtain the critical exponent $\mu = \alpha/\beta = 1.04 \pm 0.1$ in this ferromagnetic orbital-degenerate electron system. This value is consistent with the pressure-induced transition shown in the inset of Fig. 2 [27]. The obtained critical exponent ($\mu = \alpha/\beta = 1.04 \pm 0.1$) is intermediate between the typical value of the

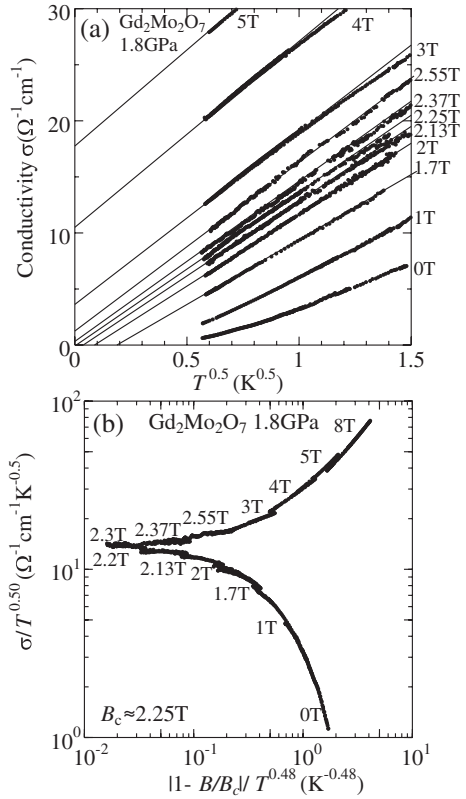

FIG. 4. (a) Conductivity σ plotted as a function of the square root of temperature $T^{0.5}$ for various magnetic fields. The magnetoconductivity was measured at 1.8 GPa. The solid lines are guides for the eye. (b) Finite-temperature scaling analysis. The data of Fig. 4(a) are fitted to the equation, $\sigma/T^{0.5} = f(|1 - B/B_c|/T^{0.48})$. The critical field B_c was estimated as 2.25 T.

Mott transition such as Cr-doped V_2O_3($\mu = 0.33$) [4] and the theoretical values ($\mu = \nu = 1.4$–1.6) expected for the genuine Anderson transition of the noninteracting electron system [11], indicating that the MI transition of $Gd_2Mo_2O_7$ possesses the mixed character of the Mott-Anderson transition. The disorder effect is added as a subtle control parameter of the metal-insulator transition governed by the strong electron-correlation effect. The importance of the electron-correlation effect has been investigated extensively for the Mott-Anderson transition in semiconductors as well [28–31].

In conclusion, the pressure-induced as well as magnetic-field induced insulator-metal transition has been investigated for the $Gd_2Mo_2O_7$ locating on the verge of the phase boundary between the ferromagnetic metal and the spin-glass Mott insulator. The geometrical frustration gives rise to the random potential for the quasiparticle state, which can be controlled by the external magnetic field. We have investigated the Mott-Anderson transition by the application of high pressure and magnetic field in this ferromagnetic orbital-degenerate electron system and obtained the critical exponent $\mu = 1.04 \pm 0.1$ by the finite-temperature scaling analysis.

The authors are grateful to Y. Taguchi, D. Hashimoto, M. Imada, N. Nagaosa, S. Watanabe, and S. Onoda for enlightening discussions. This work was supported by a Grant-in-Aid for Scientific Research from MEXT.

[1] M. Imada, A. Fujimori, and Y. Tokura, Rev. Mod. Phys. **70**, 1039 (1998).
[2] A. Georges *et al.*, Rev. Mod. Phys. **68**, 13 (1996).
[3] A. Georges *et al.*, J. Phys. IV (France) **114**, 165 (2004).
[4] P. Limelette *et al.*, Science **302**, 89 (2003). μ corresponds to $1/\delta$ for the first-order Mott transition because of $\sigma - \sigma_c \sim h1/\delta$. Here, h and δ denote the control parameter and the critical exponent, respectively.
[5] F. Kagawa *et al.*, Phys. Rev. B **69**, 064511 (2004).
[6] F. Kagawa, K. Miyagawa, and K. Kanoda, Nature (London) **436**, 534 (2005).
[7] P. A. Lee and T. V. Ramakrishnan, Rev. Mod. Phys. **57**, 287 (1985).
[8] D. Belitz and T. R. Kirkpatrick, Rev. Mod. Phys. **66**, 261 (1994).
[9] A. M. Finkelstein, Z. Phys. B **56**, 189 (1984).
[10] C. Castellani *et al.*, Phys. Rev. B **30**, 527 (1984); C. Castellani *et al.*, Phys. Rev. B **30**, 1596 (1984).
[11] K. Slevin and T. Ohtsuki, Phys. Rev. Lett. **78**, 4083 (1997). K. Slevin and T. Ohtsuki, Phys. Rev. Lett. **82**, 382 (1999); M. Henneke *et al.*, Europhys. Lett. **27**, 389 (1994); T. Kawarabayashi *et al.*, Phys. Rev. Lett. **77**, 3593 (1996).
[12] *Anderson Localization*, edited by T. Ando and H. Fukuyama (Springer-Verlag, Berlin, 1988).
[13] E. Abrahams and G. Kotliar, Science **274**, 1853 (1996).
[14] V. Dobrosavljevic and G. Kotliar, Phil. Trans. R. Soc. A **356**, 57 (1998).
[15] A. Husmann *et al.*, Science **274**, 1874 (1996).
[16] Y. Taguchi *et al.*, Science **291**, 2573 (2001).
[17] I. V. Solovyev, Phys. Rev. B **67**, 174406 (2003).
[18] T. Katsufuji *et al.*, Phys. Rev. Lett. **84**, 1998 (2000).
[19] Y. Taguchi *et al.*, Phys. Rev. B **65**, 115102 (2002).
[20] M. W. Kim *et al.*, Phys. Rev. Lett. **92**, 027202 (2004).
[21] Y. Moritomo *et al.*, Phys. Rev. B **63**, 144425 (2001).
[22] I. Kézsmárki *et al.*, Phys. Rev. Lett. **93**, 266401 (2004).
[23] K. Taniguchi *et al.*, Phys. Rev. B **70**, 100401 (2004).
[24] The details of these high-performance pressure cells will be published elsewhere.
[25] J. D. M. Champion *et al.*, Phys. Rev. B **64**, 140407 (2001).
[26] M. Imada, Phys. Rev. B **72**, 075113 (2005).
[27] The pressure value does not have enough high resolution to analyze by the finite-temperature scaling method as compared with the accuracy of the magnetic field of the control parameter. The preliminary scaling result indicates that $\alpha \approx \beta \approx 1/2$ and $\mu \approx 1$.
[28] K. M. Itoh *et al.*, J. Phys. Soc. Jpn. **73**, 173 (2004).
[29] P. Dai *et al.*, Phys. Rev. B **48**, 4941 (1993).
[30] S. Bogdanovich *et al.*, Phys. Rev. Lett. **82**, 137 (1999).
[31] T. G. Castner, Phys. Rev. Lett. **84**, 1539 (2000).